International Journal of Engineering & Technology, 7 (4) (2018) 5007-5017

International Journal of Engineering & Technology

Website: www.sciencepubco.com/index.php/IJET
doi: 10.14419/ijet. v7i4.25887
Research paper

Calculating the frequency of composite plate and composite spherical shell with different boundary conditions

Aya Adnan Yaseen1 [1], Luay S. Alansari [2] *, Mohammed Hussain Alnajem [3], Qusay S. Al-anssari [4]

[1] *Al Mansour University College, Baghdad, Iraq*
[2] *University of Kufa, College of Engineering, Department of Mechanical Engineering, Najaf, Iraq*
[3] *The Islamic University- Engineering College- Refrigeration and Air-Conditioning Techniques Department, Najaf, Iraq*
[4] *Electricity Distribution Branch in Najaf Governorate, General Electricity Distribution Company, Najaf, Iraq*
**Corresponding author E-mail: luays.alansari@uokufa.edu.iq*

Abstract

In this work, the Fourier-Ritz approach is used to calculate the natural non- dimensional frequency of composite plate and compo-site spherical shell with different arrangements of layers (cross and angle ply and symmetrical and anti-symmetrical layers) and dif-ferent boundary conditions. The Fourier-Ritz approach is the modified Fourier series in connection with a Ritz technique to de-duce the formulation based on the classical shallow shell theory. Additionally, the Finite Element method (FEM) (ANSYS Software Version 17.2) is used in this work for predicting the natural non- dimensional frequency of composite plate and composite spherical shell. The effect of (b/a) ratio on non- dimensional frequency of composite plate and composite spherical shell is studied for differ-ent layers arrangements when the boundary conditions are (CCCC) and (SSSS). The comparisons between the non- dimensional frequency results are made.

Keywords: *Fourier-Ritz Method; Finite Element Method; ANSYS, Free Vibration; Composite Spherical Shell; Composite Plate.*

1. Introduction

A shell can be defined as a three dimensional body confined by two parallel surfaces unless the thickness is varying and the distance between those surfaces is small compared with other shell parameters. Shallow shell is one of common shell structural elements and can be defined as an open shell that has small curvature (i.e. if the radii of curvature are larger than other shell parameters such as length and width). The shallow shell can be classified according to types of curvature into circular cylindrical, spherical, ellipsoidal, hyperbolic and paraboloidal or can be classified according to types of planforms into triangular, trapezoidal, rectangular, circular, and others. The shallow shells are widely used in aircraft structures, space vehicles, deep-sea engineering equipment, aerospace structures, , civil engineering applications and other fields of engineering. Several works dealt with vibration of shallow shell considering isotropic material and these researches proposed and developed various shell theories. Shell theories can be classified into three main categories:

1) Thin shallow shell theory [1-12] (e.g., classical shell theory or CST).
2) Thick shallow shell theory [13-17] (e.g., HSDT and three-dimensional (3-D) elasticity theory or higher-order shear deformation theory).
3) Moderately thick shallow shell theory [18-21] (e.g., first-order shear deformation theory or FSDT).

In additional to Shell theories, several methods of solution were proposed in these researches like numerous analytical (wave propagation method [9]), semi-analytical and numerical methods (finite element method (FEM) [19] and Rayleigh-Ritz method [3-7]). Qatu [22] has looked clearly at the natural vibration of fully free laminated composite shallow shells that are of two types triangular and trapezoidal using the five-levels -of- freedom shallow shell theory. Khdeir and Reddy [23] has added a propagated modal approach for the prediction of free and force vibration of the arches of cross- ply laminated composite shallow. Soldatos and Shu [24] have exactly predicted the stress analysis of cross-ply laminated plates and shallow shell panels with a rectangular plan-form. Reddy et al [25] and Qatu [26] have examined the wide interest in vibration actions of laminated composite shallow shells. Most of the previous studies on this subject are limited to the classical boundary conditions and their integrations (i.e., clamped, simply-supported, free and shear-diaphragm boundaries). It is obvious, in mesh free method which is based on the wavelet collocation, is used by Ferreira et al. [27] to compute the static deformation and frequencies of doubly-curved composite shells. The two kinds of vibration analysis static or free of the doubly-curved shells has been performed by Ferreira et al. [27,28] with the radial standard of the collocation features. Qatu and Asadi [29] have introduced the first understandable free vibration project of isotropic shallow shells which are subjected to arbitrary boundary circumstances of Ritz method. Fazzolari and Carrera[30] has developed a hierarchical trigonometric Ritz formulation which is related to free vibration and dynamic reaction analysis of doubly-curved anisotropic laminated shallow as well as deep shells. Guoyong Jinet el at [31] has studied a defined Fourier-Ritz approach for free vibration analysis of laminated effectively stepped shallow shells with widespread boundary conditions in the scope of first-order sheared figuration shallow shell theory. Qingshan Wang et.al [32] has finished the vibration works of composite laminated circular panels and shells with common elastic restraints revolution and also improved a connecting adequately accurate analytical procedure to achieve some beneficial results of the target problem which may be used for evaluating future researchers. The first shear distorted order shell theory is used to formulate the theoretical model. Wang et.al [33] have introduced a semi- analytical method for

Copyright © 2018 Aya Adnan Yaseen et. al. This is an open access article distributed under the Creative Commons Attribution License, which permits unrestricted use, distribution, and reproduction in any medium, provided the original work is properly cited.

feasibly graded carbon nanotubes that in return emphasized a composite shallow shells with general boundary conditions by using the Rayleigh–Ritz method. This method has used the developed Fourier series to explain the admitted function of shells, four different unique types of the doubly curved panels are studied comprising with the cylindrical shallow, spherical shell, hyperbolic paraboloid shallow and flat plate. The arbitrary boundary conditions are adopted by presenting the artificial spring boundary technique. In this work, the Fourier-Ritz approach and finite element method (FEM) are used to calculate the natural frequency of composite plate and composite spherical shell with different arrangements of layers (cross and angle ply and symmetrical and anti-symmetrical layers). The effect of (b/a) ratio on frequency is studied.

2. Governing equations and solution

Vibration problems such as classical laminated thin shallow shell theory (CSST), higher order shear deformation shallow shell theory (HSST) and first order shear deformation theory (FSDT). In this work, the classical shallow shell theory (CSST) is used in order to study the free vibration of isotropic and orthotropic spherical shell with different boundary conditions.
For the case of coordinates of principal curvature, the reduced equations of motion for the laminated shallow shell can be written in terms of force and moment resultants as [26]:

∂N〗_x/∂x+〖∂N〗_xy/∂y+q_x=-I_s (∂^2 u)/(∂^2 t)

Generally, the reduced equations of motion for the laminated shallow shell can be written in terms of displacement and rotation components as [26, 34, and 35]:

$$\left\{\begin{bmatrix}\mathcal{L}_{11} & \mathcal{L}_{12} & \mathcal{L}_{13}\\ \mathcal{L}_{21} & \mathcal{L}_{22} & \mathcal{L}_{23}\\ \mathcal{L}_{31} & \mathcal{L}_{32} & \mathcal{L}_{33}\end{bmatrix} - \omega^2\begin{bmatrix}I_s & 0 & 0\\ 0 & I_s & 0\\ 0 & 0 & I_s\end{bmatrix}\right\}\begin{bmatrix}u\\ v\\ w\end{bmatrix} = \begin{bmatrix}q_x\\ q_y\\ q_z\end{bmatrix} \quad (1)$$

Where $\mathcal{L}_{ij}$ are coefficients of the linear operator and can be written as:

$$\mathcal{L}_{11} = \mathcal{A}_{11}\frac{\partial^2}{\partial x^2} + 2\mathcal{A}_{16}\frac{\partial^2}{\partial x\,\partial y} + \mathcal{A}_{66}\frac{\partial^2}{\partial y^2}$$

$$\mathcal{L}_{22} = \mathcal{A}_{66}\frac{\partial^2}{\partial x^2} + 2\mathcal{A}_{26}\frac{\partial^2}{\partial x\,\partial y} + \mathcal{A}_{22}\frac{\partial^2}{\partial y^2}$$

$$\mathcal{L}_{33} = 2\left\{\left(\frac{\mathcal{B}_{11}}{R_x} + \frac{\mathcal{B}_{12}}{R_y} + \frac{2\mathcal{B}_{16}}{R_{xy}}\right)\frac{\partial^2}{\partial x^2} + 2\left(\frac{\mathcal{B}_{16}}{R_x} + \frac{\mathcal{B}_{26}}{R_y} + \frac{2\mathcal{B}_{66}}{R_{xy}}\right)\frac{\partial^2}{\partial x\,\partial y} + \left(\frac{\mathcal{B}_{12}}{R_x} + \frac{\mathcal{B}_{22}}{R_y} + \frac{\mathcal{B}_{26}}{R_{xy}}\right)\frac{\partial^2}{\partial y^2}\right\} - \left\{\frac{\mathcal{A}_{11}}{R_x^2} + \frac{2\mathcal{A}_{12}}{R_xR_y} + \frac{\mathcal{A}_{22}}{R_y^2} + 4\left(\frac{\mathcal{A}_{16}}{R_xR_{xy}} + \frac{\mathcal{A}_{26}}{R_yR_{xy}} + \frac{\mathcal{A}_{66}}{R_{xy}^2}\right)\right\} - \mathcal{D}_{11}\frac{\partial^4}{\partial x^4} - 4\mathcal{D}_{16}\frac{\partial^4}{\partial x^3\,\partial y} - 2(\mathcal{D}_{12} + 2\mathcal{D}_{66})\frac{\partial^4}{\partial x^2\,\partial y^2} - 4\mathcal{D}_{26}\frac{\partial^4}{\partial x\,\partial y^3} - \mathcal{D}_{22}\frac{\partial^4}{\partial y^4}$$

$$\mathcal{L}_{12} = \mathcal{L}_{21} = \mathcal{A}_{16}\frac{\partial^2}{\partial x^2} + (\mathcal{A}_{12} + \mathcal{A}_{66})\frac{\partial^2}{\partial x\,\partial y} + \mathcal{A}_{26}\frac{\partial^2}{\partial y^2}$$

$$\mathcal{L}_{13} = -\mathcal{L}_{31} = \left(\frac{\mathcal{A}_{11}}{R_x} + \frac{\mathcal{A}_{12}}{R_y} + \frac{2\mathcal{A}_{16}}{R_{xy}}\right)\frac{\partial}{\partial x} + \left(\frac{\mathcal{A}_{16}}{R_x} + \frac{\mathcal{A}_{26}}{R_y} + \frac{2\mathcal{A}_{66}}{R_{xy}}\right)\frac{\partial}{\partial y} - \mathcal{B}_{11}\frac{\partial^3}{\partial x^3} + \mathcal{B}_{26}\frac{\partial^3}{\partial y^3} + 3\mathcal{B}_{16}\frac{\partial^3}{\partial x^2\,\partial y} + (\mathcal{B}_{12} + 2\mathcal{B}_{66})\frac{\partial^3}{\partial x\,\partial y^2}$$

$$\mathcal{L}_{23} = -\mathcal{L}_{32} = \left(\frac{\mathcal{A}_{16}}{R_x} + \frac{\mathcal{A}_{26}}{R_y} + \frac{2\mathcal{A}_{66}}{R_{xy}}\right)\frac{\partial}{\partial x} + \left(\frac{\mathcal{A}_{12}}{R_x} + \frac{\mathcal{A}_{22}}{R_y} + \frac{2\mathcal{A}_{26}}{R_{xy}}\right)\frac{\partial}{\partial y} - \mathcal{B}_{16}\frac{\partial^3}{\partial x^3} + \mathcal{B}_{22}\frac{\partial^3}{\partial y^3} + (\mathcal{B}_{12} + 2\mathcal{B}_{66})\frac{\partial^3}{\partial x^2\,\partial y} + 3\mathcal{B}_{26}\frac{\partial^3}{\partial x\,\partial y^2}$$

The general boundary conditions of thin shallow shell are considered here in combination are expressed as:

$$1 - At\ x = 0 \rightarrow \begin{cases} \mathcal{N}_x + \dfrac{\mathcal{M}_x}{R_x} - \mathcal{K}_{x0}^{u}u = 0\\ \mathcal{N}_x + \dfrac{\mathcal{M}_{xy}}{R_x} - \mathcal{K}_{x0}^{v}v = 0\\ \mathcal{Q}_x + \dfrac{\partial\mathcal{M}_{xy}}{\partial y} - \mathcal{K}_{x0}^{w}w = 0\\ -\mathcal{M}_x - \mathcal{K}_{x0}^{w}w\dfrac{\partial w}{\partial x} = 0 \end{cases} \quad (2)$$

$$2 - At\ x = a \rightarrow \begin{cases} \mathcal{N}_x + \dfrac{\mathcal{M}_x}{R_x} - \mathcal{K}_{xa}^{u}u = 0\\ \mathcal{N}_{xy} + \dfrac{\mathcal{M}_{xy}}{R_y} - \mathcal{K}_{xa}^{v}v = 0\\ \mathcal{Q}_x + \dfrac{\partial\mathcal{M}_{xy}}{\partial y} - \mathcal{K}_{xa}^{w}w = 0\\ -\mathcal{M}_x - \mathcal{K}_{xa}^{w}w\dfrac{\partial w}{\partial x} = 0 \end{cases} \quad (3)$$

$$3 - At\ y = 0 \rightarrow \begin{cases} \mathcal{N}_{xy} + \dfrac{\mathcal{M}_{xy}}{R_x} - \mathcal{K}_{y0}^{u}u = 0\\ \mathcal{N}_y + \dfrac{\mathcal{M}_y}{R_y} - \mathcal{K}_{y0}^{v}v = 0\\ \mathcal{Q}_y + \dfrac{\partial\mathcal{M}_{xy}}{\partial x} - \mathcal{K}_{y0}^{w}w = 0\\ -\mathcal{M}_y - \mathcal{K}_{y0}^{w}w\dfrac{\partial w}{\partial y} = 0 \end{cases} \quad (4)$$

$$4 - At\ y = b \rightarrow \begin{cases} \mathcal{N}_{xy} + \dfrac{\mathcal{M}_{xy}}{R_x} - \mathcal{K}_{yb}^{u}u = 0\\ \mathcal{N}_y + \dfrac{\mathcal{M}_y}{R_y} - \mathcal{K}_{yb}^{v}v = 0\\ \mathcal{Q}_y + \dfrac{\partial\mathcal{M}_{xy}}{\partial x} - \mathcal{K}_{yb}^{w}w = 0\\ -\mathcal{M}_y - \mathcal{K}_{yb}^{w}w\dfrac{\partial w}{\partial y} = 0 \end{cases} \quad (5)$$

In order to solving equations of motion, modified Fourier method is used to derive these displacement functions and the following displacement functions are assumed:

$$u(x.y.t) = U(x.y)e^{j\omega t} = \left\{\begin{matrix}\sum_{m=0}^{\infty}\sum_{n=0}^{\infty}\mathcal{A}_{mn}\cos\lambda_m x\cos\lambda_n y\\ +\sum_{\ell=1}^{2}\left\{\sum_{n=0}^{\infty}\mathcal{A}_{\ell n}^{a}\zeta_\ell(x)\cos\lambda_n y + \sum_{n=0}^{\infty}\mathcal{A}_{\ell m}^{b}\zeta_\ell(y)\cos\lambda_m x\right\}\end{matrix}\right\}e^{j\omega t} \quad (6)$$

$$v(x.y.t) = \mathrm{V}(x.y)e^{j\omega t} = \left\{\begin{matrix}\sum_{m=0}^{\infty}\sum_{n=0}^{\infty}\mathcal{B}_{mn}\cos\lambda_m \mathrm{x}\cos\lambda_n \mathrm{y}\\ +\sum_{\ell=1}^{2}\left\{\sum_{n=0}^{\infty}\mathcal{B}_{\ell n}^{a}\zeta_\ell(\mathrm{x})\cos\lambda_{\mathrm{n}}\mathrm{y} + \sum_{n=0}^{\infty}\mathcal{B}_{\ell m}^{b}\zeta_\ell(\mathrm{y})\cos\lambda_{\mathrm{m}}\mathrm{x}\right\}\end{matrix}\right\}e^{j\omega t} \quad (7)$$

$$w(x.y.t) = W(x.y)e^{j\omega t} = \left\{\begin{matrix}\sum_{m=0}^{\infty}\sum_{n=0}^{\infty}\mathcal{C}_{mn}\cos\lambda_m \mathrm{x}\cos\lambda_n \mathrm{y}\\ +\sum_{\ell=1}^{4}\left\{\sum_{n=0}^{\infty}\mathcal{C}_{\ell n}^{a}\xi_\ell(\mathrm{x})\cos\lambda_{\mathrm{n}}\mathrm{y} + \sum_{n=0}^{\infty}\mathcal{C}_{\ell m}^{b}\xi_\ell(\mathrm{y})\cos\lambda_{\mathrm{m}}\mathrm{x}\right\}\end{matrix}\right\}\mathrm{e}^{\mathrm{j}\omega\mathrm{t}} \quad (8)$$

Where:
$\mathcal{A}_{mn}$, $\mathcal{B}_{mn}$ and $\mathcal{C}_{mn}$ are the Fourier coefficients.
$\mathcal{A}_{\ell n}^{a}$, $\mathcal{A}_{\ell m}^{b}$, $\mathcal{B}_{\ell n}^{a}$, $\mathcal{B}_{\ell n}^{b}$, $\mathcal{C}_{\ell n}^{a}$ and $\mathcal{C}_{\ell n}^{b}$ are the coefficients of the supplementary terms.
$\lambda_m = m\pi/a$ and $\lambda_n = n\pi/b$.
All these coefficients are treated individually as an independent set of generalized coordinates and they are required to be determined. ω is the natural frequency of the shell.
While $\xi_\ell(x)$ and $\xi_\ell(y)$ are auxiliary functions and the values of ℓ are (1 and 2) for in-plane displacements $(u.v)$ whereas the values of ℓ are (1, 2 , 3 and 4) for transverse vibration displacement w. These auxiliary functions can be written as:

$$\zeta_1(s) = s\left(\frac{s}{r} - 1\right)^2.\ \zeta_2(s) = \frac{s^2}{r}\left(\frac{s}{r} - 1\right)^2$$

$$\xi_1(s) = \frac{-9r}{4\pi}\sin\left(\frac{\pi s}{2r}\right) - \frac{r}{12\pi}\sin\left(\frac{3\pi s}{2r}\right)$$

$$\xi_2(s) = \frac{-9r}{4\pi}\cos\left(\frac{\pi s}{2r}\right) - \frac{r}{12\pi}\cos\left(\frac{3\pi s}{2r}\right)$$

$$\xi_3(s) = \frac{r^3}{\pi^3}\sin\left(\frac{\pi s}{2r}\right) - \frac{r^3}{3\pi^3}\sin\left(\frac{3\pi s}{2r}\right)$$

$$\xi_4(s) = \frac{-r^3}{\pi^3}\cos\left(\frac{\pi s}{2r}\right) - \frac{r^3}{3\pi^3}\cos\left(\frac{3\pi s}{2r}\right)$$

Where: $s = \mathrm{x.y}$, $r = \mathrm{a.b}$,

$$\xi_1'(0) = \xi_2'(r) = \xi_3'''(0) = \xi_4'''(r) = \zeta_1'(0) = \zeta_1'(r) = 1.$$

Using Raleigh–Ritz method to carry out minimization of the Lagrangian function ($\mathcal{L}$) by differentiation the Lagrangian function ($\mathcal{L}$) with respect to constants found in equations (24)(i.e. constants $\mathcal{A}_{mn}$, $\mathcal{A}^{a}_{\ell n}$, $\mathcal{A}^{b}_{\ell m}$, $\mathcal{B}_{mn}$, $\mathcal{B}^{a}_{\ell n}$, $\mathcal{B}^{b}_{\ell n}$, $\mathcal{C}_{mn}$, $\mathcal{C}^{a}_{\ell n}$ and $\mathcal{C}^{b}_{\ell n}$).
For Free vibration, the solutions are truncated numerically to M and N. Therefore, equation (1) can be written as:

$$(\mathbb{K} - \omega^2 \mathbb{M})\mathbb{G} = 0 \tag{9}$$

Where, $\mathbb{M}$ and $\mathbb{K}$ are mass and stiffness matrices of the shallow shell respectively. They are both symmetric and are expressed as: expressed as:

$$\mathbb{M} = \begin{bmatrix} \mathbb{M}_{11} & \mathbb{M}_{12} & \mathbb{M}_{13} & \cdots & \mathbb{M}_{19} \\ \mathbb{M}^{T}_{12} & \mathbb{M}^{T}_{22} & \mathbb{M}^{T}_{23} & \cdots & \mathbb{M}_{29} \\ \mathbb{M}^{T}_{13} & \mathbb{M}^{T}_{23} & \mathbb{M}^{T}_{33} & \cdots & \mathbb{M}_{39} \\ \vdots & \vdots & \vdots & \ddots & \vdots \\ \mathbb{M}^{T}_{19} & \mathbb{M}^{T}_{29} & \mathbb{M}^{T}_{39} & \cdots & \mathbb{M}_{99} \end{bmatrix} \tag{10}$$

And

$$\mathbb{K} = \begin{bmatrix} \mathbb{K}_{11} & \mathbb{K}_{12} & \mathbb{K}_{13} & \cdots & \mathbb{K}_{19} \\ \mathbb{K}^{T}_{12} & \mathbb{K}^{T}_{22} & \mathbb{K}^{T}_{23} & \cdots & \mathbb{K}_{29} \\ \mathbb{K}^{T}_{13} & \mathbb{K}^{T}_{23} & \mathbb{K}^{T}_{33} & \cdots & \mathbb{K}_{39} \\ \vdots & \vdots & \vdots & \ddots & \vdots \\ \mathbb{K}^{T}_{19} & \mathbb{K}^{T}_{29} & \mathbb{K}^{T}_{39} & \cdots & \mathbb{K}_{99} \end{bmatrix} \tag{11}$$

The detail expression for these matrices are given in Appendix A, G is the vector of the expanded and supplemented coefficients, is written as:

$$\mathbb{G} = [\mathbb{G}^{u} \quad \mathbb{G}^{v} \quad \mathbb{G}^{w}]^{T} \tag{12}$$

Where;

$$\mathbb{G}^{u}[\mathcal{A}_{00}.\ldots.\mathcal{A}_{mn}.\ldots.\mathcal{A}_{MN}.\mathcal{A}^{a}_{10}.\ldots.\ldots.\mathcal{A}^{a}_{2N}.\mathcal{A}^{b}_{10}.\ldots\mathcal{A}^{b}_{\ell m}.\ldots.\mathcal{A}^{b}_{2M}]$$
$$\mathbb{G}^{v}[\mathcal{B}_{00}.\ldots.\mathcal{B}_{mn}.\ldots.\mathcal{B}_{MN}.\mathcal{B}^{a}_{10}.\ldots.\ldots.\mathcal{B}^{a}_{\ell n}.\ldots.\mathcal{B}^{b}_{10}.\ldots.\mathcal{B}^{b}_{\ell m}.\ldots.\mathcal{B}^{b}_{2M}]$$

$$\mathbb{G}^{w}[\mathcal{C}_{00}.\ldots.\mathcal{C}_{mn}.\ldots.\mathcal{C}_{MN}.\mathcal{C}^{a}_{10}.\ldots.\mathcal{C}^{a}_{\ell n}.\ldots.\mathcal{C}^{a}_{4N}.\mathcal{C}^{b}_{10}.\ldots.\mathcal{C}^{b}_{\ell m}.\ldots.\mathcal{C}^{b}_{4M}]$$

The characteristic equation of the generalized Eigen value problem is used to determine the all the natural frequencies and corresponding modes. Once the coefficients of $\mathbb{G}$ are determined, the displacement functions are obtained by substituting these coefficients in the standard displacement functions. Mode shape is constructed from these displacement functions.

3. Finite element model

In addition to Fourier-Ritz method, two – dimensional finite element model using ANSYS software (version 17.2) is built. In this model, the Shell element (SHELL281) is used. The number of elements is about (20000) element and the number of nodes is about (70000) node. The suitable size of element is tested in order to minimize the error in calculation.

4. Validation

In this work, MATLAB code is built for the present composite plate and spherical shell and the MATLAB code is examined by studying its validity for free vibration frequencies of isotropic and composite plates and spherical shell. The validation of this work can be divided into:
1- Isotropic Plate: In this case, the non – dimensional frequency parameters of an isotropic material with Modulus of Elasticity (E) = 1 (GPas.) and Poisson Ratio (μ) =0.3 are calculated using present and finite element method and compared with the non – dimensional frequency parameters calculated by Wang [36] who used B-spline Rayleigh Ritz method. Table (1) shows the comparison among these three methods for two types of boundary conditions (all edges are simply supported (SSSS) and all edges are clamped (CCCC)). Where the non – dimensional frequency parameter is:

$$\varpi = \omega a^2 / \pi^2 \sqrt{\rho h / D}$$

Where;

$$D = Eh^3 / 12(1 - \mu^2)$$

and ρ is the Density.

Table 1: Comparison Among the Values of Non-Dimensional Frequency Parameter Calculating by Different Methods for Isotropic Plate with Two Types of Supporting When Modulus of Elasticity (E) =1 Gpas. and Poison Ratio (μ) =0.3

Mode Number	SSSS Present	ANSYS	Wang [36]	CCCC Present	ANSYS	Wang [36]
1	1.999	1.9983	2	3.643	3.6446	3.6461
2	4.996	4.9966	5	7.525	7.4333	7.4364
3	4.996	4.9966	5	7.525	7.4333	7.4364
4	7.989	7.9932	8	10.953	10.9597	10.9647
5	10	9.9942	10	13.324	13.3258	13.3321
6	10	9.9942	10	13.388	13.38968	13.3321
7	12.987	12.9893	13	16.69	16.7106	16.7183
8	12.987	12.9893	13	16.69	16.7106	16.7183

The maximum absolute error percentage between results of present method and that calculating by Wang [36] is (0.1375%) in (SSSS) supporting and (1.19 %) in (CCCC) supporting. In the other hand, the maximum absolute error percentage between results of Finite Element method (FEM) and that calculating by Wang [36] is (0.0823%) in (SSSS) supporting and (0.04725%) in (CCCC) supporting.
2- Orthotropic Plate: In this case, the non – dimensional frequency parameters of two types of orthotropic materials and these types are cross ply and angle ply. Table (2) shows the comparison among the non – dimensional frequency parameters calculating by the three methods (present, finite element and B-spline Rayleigh Ritz method) for two types of boundary conditions (all edges are simply supported (SSSS) and all edges are clamped (CCCC)) when the symmetrical cross play composite plate [0o/90o/0o/ 90o/0o] is used. For anti-symmetrical cross play composite plate [0o/90o/0o/ 90o], Table (3) shows the comparison among the non – dimensional frequency parameters calculating by the three methods for two types of boundary conditions. In this case , the non – dimensional frequency parameter is:

$$\varpi = \omega a^2 / \pi^2 h \sqrt{\rho / E_T}$$

And the mechanical properties of orthotropic material are:

E2 = 1 GPas., E1 = 40*E2, G12 = 0.6*E2, G13 = G23 = 0.5*E2, μ12 = μ13 = μ23 = 0.25.

From Table (2), the maximum absolute error percentages between results of present method and that calculating by Wang [36] are (2.286%) and (2.3%) in (SSSS) and (CCCC) respectively and appeared in eighth mode. Also, the maximum absolute error percentages between results of Finite Element method and that calculating by Wang [36] are (0.07982 %) and (0.1023 %) in (SSSS) and (CCCC) respectively. In Table (3), the maximum absolute error percentages between results of present method and that calculating by Wang [36] are (6.216%) and (1.4715%) in (SSSS) and (CCCC) respectively and the maximum absolute error percentages between results of Finite Element method and that calculating by Wang [36] are (6.682%) and (0.0835%) in (SSSS) and (CCCC) respectively.

Table 2: Comparison Among the Values of Non-Dimensional Frequency Parameter Calculating by Different Methods for Cross Ply Composite Plate [0°/90°/0°/ 90°/0°] with Two Types of Supporting when (E2 = 1

Gpas., E1 = 40*E2, G12 = 0.6*E2, G13 = G23 = 0.5*E2, μ12 = μ13 = μ23 = (0.25).

Mode Number	SSSS Present	ANSYS	Wang [36]	CCCC Present	ANSYS	Wang [36]
1	1.9093	1.9131	1.914	4.2266	4.2354	4.2378
2	3.9616	3.9724	3.974	6.668	6.6875	6.6913
3	6.584	6.653	6.657	10.335	10.4434	10.4511
4	7.581	7.6517	7.656	11.324	11.4294	11.4372
5	8.104	8.1464	8.151	11.714	11.7756	11.7839
6	10.539	10.6182	10.625	15.007	15.1324	15.1435
7	14.169	14.176	14.186	18.162	18.1713	18.1899
8	14.446	14.7722	14.784	19.692	20.1368	20.1565

Table 3: Comparison among the Values of Non-Dimensional Frequency Parameter Calculating by Different Methods for Cross Ply Composite Plate [0º/90º/0º/ 90º] with Two Types of Supporting when (E2 = 1, Gpas., E1 = 40*E2, G12 = 0.6*E2, G13 = G23 = 0.5*E2, μ12 = μ13 = μ23 = 0.25)

Mode Number	SSSS Present	ANSYS	Wang [36]	CCCC Present	ANSYS	Wang [36]
1	1.8702	1.8795	1.7539	3.81156	3.8664	3.8685
2	5.037	5.0396	5.009	7.91201	8.0035	8.0083
3	5.037	5.0396	5.009	7.91201	8.0035	8.0083
4	6.9661	7.0470	7.0154	10.6246	10.7648	10.7721
5	10.922	10.992	10.890	14.8487	14.9275	14.949
6	10.967	10.998	10.890	14.8451	14.9416	16.7215
7	12.194	12.201	12.093	16.6194	16.7076	16.7215
8	12.194	12.201	12.093	16.6194	16.7076	16.7215

In angle ply composite plate, two types of angle play composite plates were used. The first one was symmetrical angle ply composite plate [45º/-45º/45º/-45º/45º] and Table (4) shows the comparison among the non – dimensional frequency parameters calculating by the three methods for (SSSS) and (CCCC).(1.597%) was the maximum absolute error percentage between results of present method and that calculating by Wang [36] in (SSSS) and (CCCC). Also, the maximum absolute error percentages between results of Finite. Element method and that calculating by Wang [36] were (0.4026%) in (SSSS) and (0.5966%) in (CCCC). The second type of angle ply was anti-symmetrical angle ply composite plate [45º/-45º/45º/-45º] and Table (5) shows the comparison between the three calculating methods. The maximum absolute error percentage between results of present method and that calculating by Wang [36] in (SSSS) and (CCCC) were (1.1177%) and (1.3896%). Also, the maximum absolute error percentage between results of FEM and that calculating by Wang [36] in (SSSS) and (CCCC) were (1.177%) and (0.10991%).

Table 4: Comparison among the Values of Non-Dimensional Frequency Parameter Calculating by Different Methods for Angle Ply Composite Plate [45º/-45º/45º/-45o/45º] with Two Types of Supporting When (E2 = 1 Gpas., E1 = 40*E2, G12 = 0.6*E2, G13 = G23 = 0.5*E2, μ12 = μ13 = μ23 = 0.25)

Mode Number	SSSS Present	ANSYS	Wang [36]	CCCC Present	ANSYS	Wang [36]
1	2.426	2.4242	2.434	3.909	3.8986	3.922
2	4.956	4.977	4.986	7.103	7.1418	7.1464
3	6.127	6.1587	6.182	8.383	8.4526	8.4585
4	8.41	8.4692	8.487	11.109	11.203	11.211
5	10.136	10.236	10.254	13.168	13.311	13.321
6	11.466	11.603	11.646	14.507	14.729	14.742
7	12.669	12.798	12.826	15.93	16.113	16.127
8	15.025	15.185	15.217	18.577	18.795	18.814

Table 5: Comparison among the Values of Non-Dimensional Frequency Parameter Calculating by Different Methods for Angle Ply Composite Plate [45º/-45º/45º/-45º] with Two Types of Supporting when (E2 = 1 Gpas., E1 = 40*E2, G12 = 0.6*E2, G13 = G23 = 0.5*E2, μ12 = μ13 = μ23 = 0.25)

Mode Number	SSSS Present	ANSYS	Wang [36	CCCC Present	ANSYS	Wang [36]
1	2.4726	2.4849	2.4798	3.6788	3.7318	3.7341
2	5.5156	5.5257	5.4618	7.4066	7.4859	7.4912
3	5.5156	5.5257	5.4618	7.4066	7.4859	7.4912
4	9.5402	9.6511	9.6458	11.852	12.008	12.019
5	9.9462	10.01	10.027	12.771	12.838	12.849
6	10.132	10.161	10.141	12.820	12.904	12.915
7	15.033	15.041	15.008	17.973	18.069	18.089
8	15.033	15.041	15.008	17.973	18.069	18.089

Table 5: Comparison among the Values of Non-Dimensional Frequency Parameter Calculating by Different Methods for Angle Ply Composite Plate [45º/-45º/45º/-45º] with Two Types of Supporting when (E2 = 1 Gpas., E1 = 40*E2, G12 = 0.6*E2, G13 = G23 = 0.5*E2, μ12 = μ13 = μ23 = 0.25)

Mode Number	SSSS Present	ANSYS	Wang [36]	CCCC Present	ANSYS	Wang [36]
1	2.4726	2.4849	2.4798	3.6788	3.7318	3.7341
2	5.5156	5.5257	5.4618	7.4066	7.4859	7.4912
3	5.5156	5.5257	5.4618	7.4066	7.4859	7.4912
4	9.5402	9.6511	9.6458	11.852	12.008	12.019
5	9.9462	10.01	10.027	12.771	12.838	12.849
6	10.132	10.161	10.141	12.820	12.904	12.915
7	15.033	15.041	15.008	17.973	18.069	18.089
8	15.033	15.041	15.008	17.973	18.069	18.089

From the previous comparisons, excellent agreements can be noted be-tween the present method and FEM with B-spline Rayleigh Ritz method.

5. Results and discussion

In this work, effect of aspect ratio were studied for composite plates and composite spherical shells considering direction of ply (cross and angle ply) and the number of plies (symmetric and anti-symmetric plies) when the supporting conditions are (SSSS) and (CCCC). The mechanical properties of orthotropic material are: E2 = 2 GPas., E1 = 15*E2, G12 G13 = G23 = 0.5*E2, μ12 = μ13 = μ23 = 0.25 and the density is 1500 kg/m^3.

1) Composite plate: Fig.(1) shows the comparison between the non-dimensional frequency parameters of the first and second mode of the symmetrical Cross Ply Composite Plate

[0o/90o/0o/90o/0o] due to change in aspect ratio (b/a Ratio) when the supporting conditions is (CCCC).

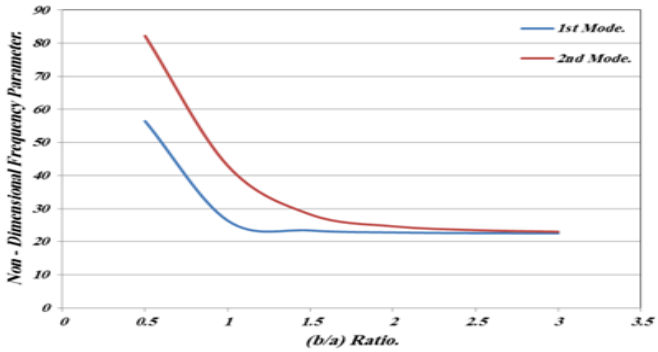


Fig. 1: The Comparison between the First and Second Non-Dimensional Frequency Parameter Due to Change In (B/A) Ratio of Cross Ply Composite Plate [0º/90º/0º/90º/0º] with CCCC Supporting.

When aspect ratio increases, the non-dimensional frequency parameter of the first and second mode will be closed to each other and this appears also in Fig. (2).

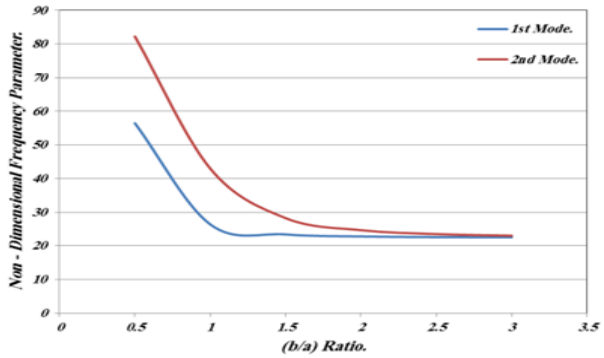


Fig. 2: The Comparison between the First and Second Non-Dimensional Frequency Parameter Due to Change in (B/A) Ratio of Cross Ply Composite Plate [0º/90º/0º/90º/0º] With SSSS Supporting.

when the supporting conditions is (SSSS) and for the same composite plate. Generally, the non-dimensional frequency parameter of (CCCC) is larger than that of (SSSS) for the first and second mode as shown in Fig.(3) and Fig.(4).

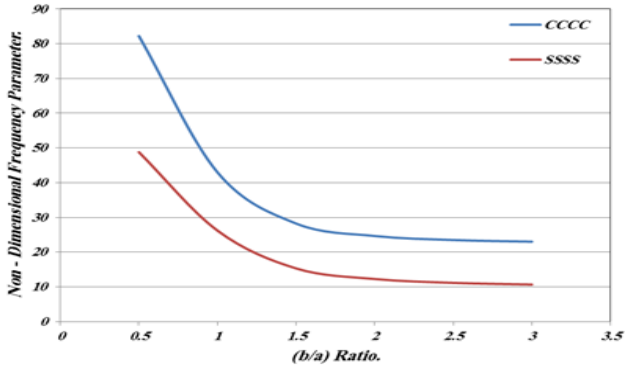


Fig. 3: The Comparison between the First Non-Dimensional Frequency Parameter of CCCC and SSSS Supporting Due to Change In (B/A) Ratio of Cross Ply Composite Plate [0º/90º/0º/90º/0º].

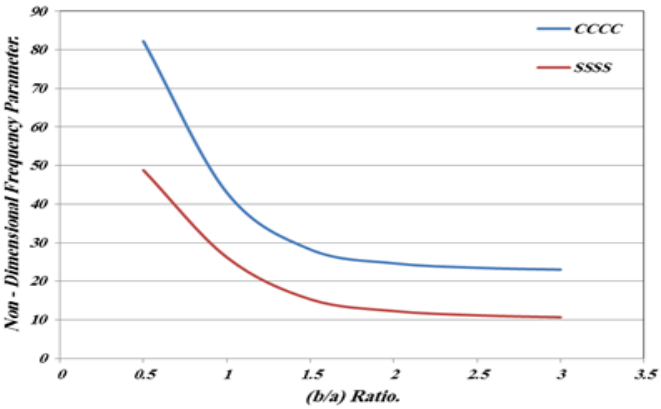


Fig. 4: The Comparison between the Second Non-Dimensional Frequency Parameter of CCCC And SSSS Supporting Due to Change in (B/A) Ratio Of Cross Ply Composite Plate [0º/90º/0º/90º/0º].

Also, the aspect ratio in the first mode is larger than that in second mode (see the decreasing rate). For the anti-symmetrical Cross Ply Composite Plate [0º/90º/0º/90º], Fig.(5) and Fig.(6) show the comparison between the non-dimensional frequency parameters of the first and second mode due to change in aspect ratio (b/a Ratio) when the supporting conditions is (CCCC) and (SSSS) respectively for the same composite plate.

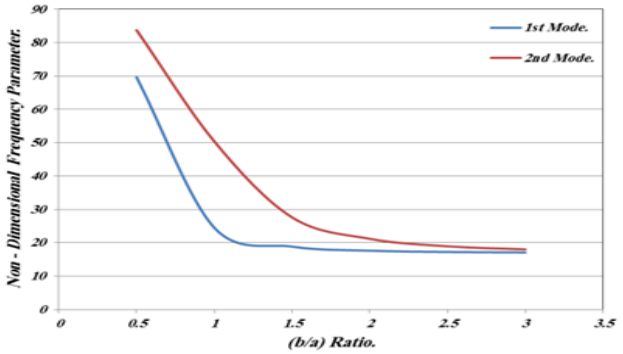


Fig. 5: The Comparison between the First and Second Non-Dimensional Frequency Parameter Due to Change In (B/A) Ratio of Cross Ply Composite Plate [0º/90º/0º/90º] with CCCC Supporting.

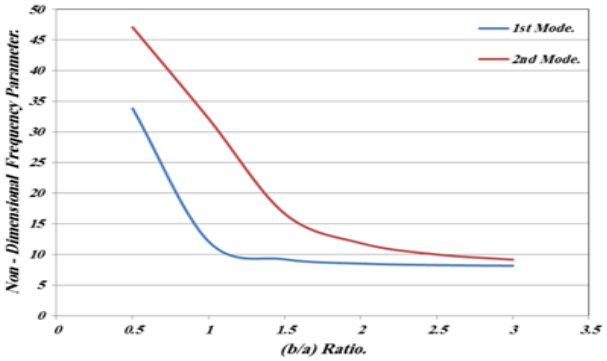


Fig. 6: The Comparison between the First and Second Non-Dimensional Frequency Parameter Due to Change in (B/A) Ratio of Cross Ply Composite Plate [0º/90º/0º/90º] with SSSS Supporting.

Fig. (7) and Fig. (8) show the comparison between the supporting condition for the first and second mode respectively. The aspect ratio in the first mode is larger than that in second mode (see the decreasing rate in Fig. (7) and Fig. (8)).

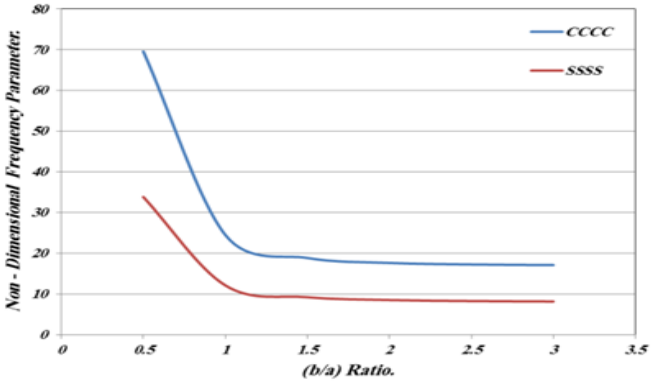


Fig. 7: The Comparison between the First Non-Dimensional Frequency Parameter of CCCC and SSSS Supporting Due to Change in (B/A) Ratio Of Cross Ply Composite Plate [0º/90º/0º/90º].

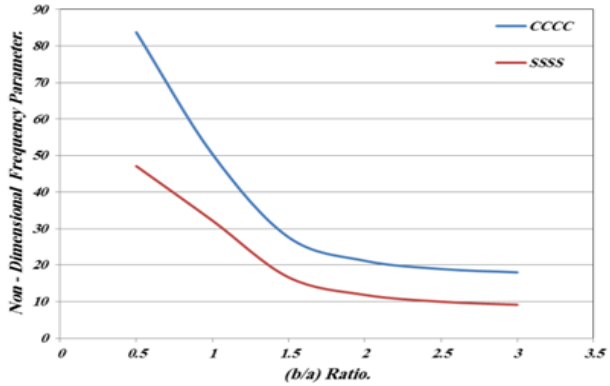


Fig. 8: The Comparison between the Second Non-Dimensional Frequency Parameter of CCCC And SSSS Supporting Due to Change in (B/A) Ratio of Cross Ply Composite Plate [0º/90º/0º/90º].

For the symmetrical angle Ply Composite Plate [45º/-45º/45º/-45º/45º], Fig. (9) and Fig.(10) show the comparison between the non-dimensional frequency parameters of the first and second mode due to change in aspect ratio (b/a Ratio) when the supporting conditions is (CCCC) and (SSSS) respectively for the same composite plate.

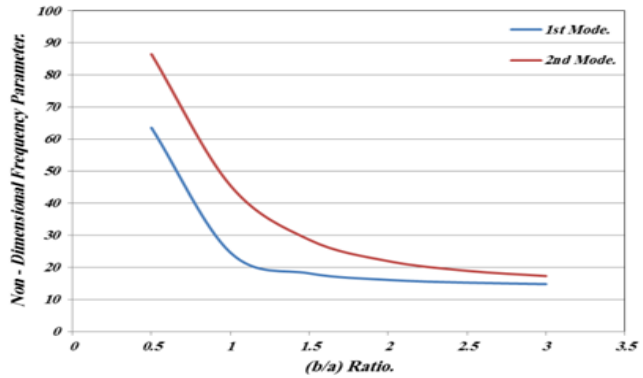


Fig. 9: The Comparison between the First and Second Non-Dimensional Frequency Parameter Due to Change in (B/A) Ratio of Angle Ply Composite Plate [45º/-45º/45º/-45º/45º] with CCCC Supporting.

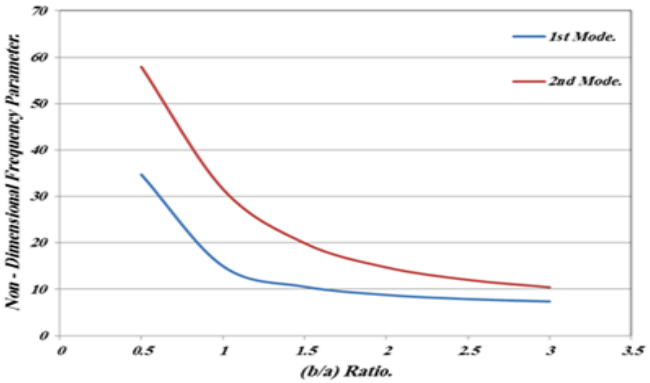


Fig. 10: The Comparison between the First and Second Non-Dimensional Frequency Parameter Due to Change in (B/A) Ratio of Angle Ply Composite Plate [45º/-45º/45º/-45º/45º] with SSSS Supporting.

The aspect ratio in the first mode is larger than that in second mode (see the decreasing rate in Fig. (11) and Fig. (12)). The same comparisons can be seen in Fig. (13)-Fig. (16) for the anti-symmetrical angle Ply Composite Plate [45º/-45º/45º/-45º].

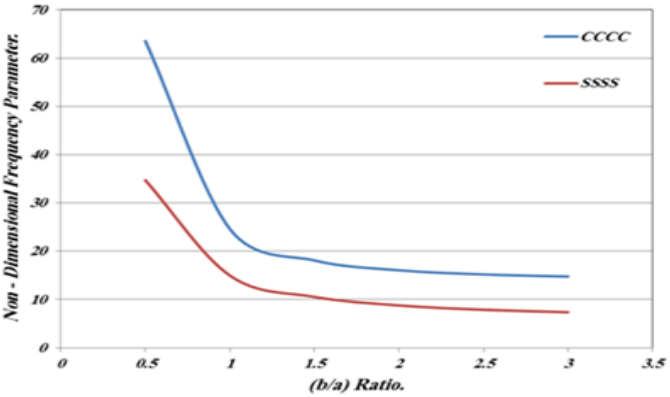


Fig. 11: The Comparison between the First Non-Dimensional Frequency Parameter of CCCC and SSSS Supporting Due to Change in (B/A) Ratio of Angle Ply Composite Plate [45º/-45º/45º/-45º/45º].

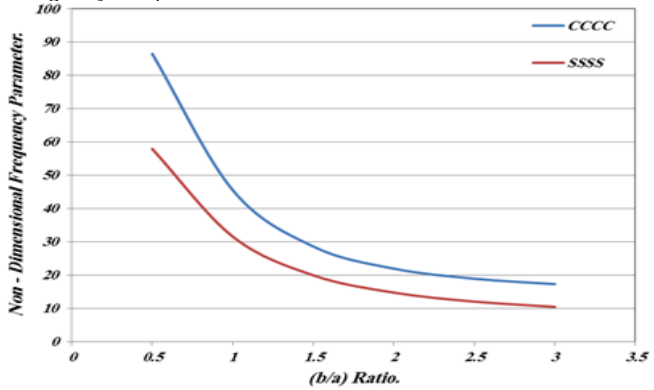


Fig. 12: The Comparison between the Second Non-Dimensional Frequency Parameter of CCCC And SSSS Supporting Due to Change in (B/A) Ratio of Angle Ply Composite Plate [45º/-45º/45º/-45º/45º].

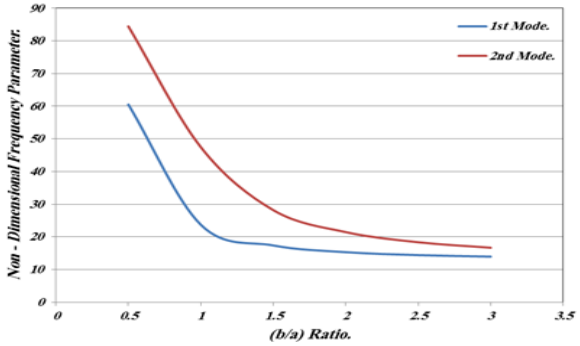


Fig. 13: The Comparison between the First and Second Non-Dimensional Frequency Parameter Due to Change in (B/A) Ratio of Angle Ply Composite Plate [45º/-45º/45º/-45º] With CCCC Supporting.

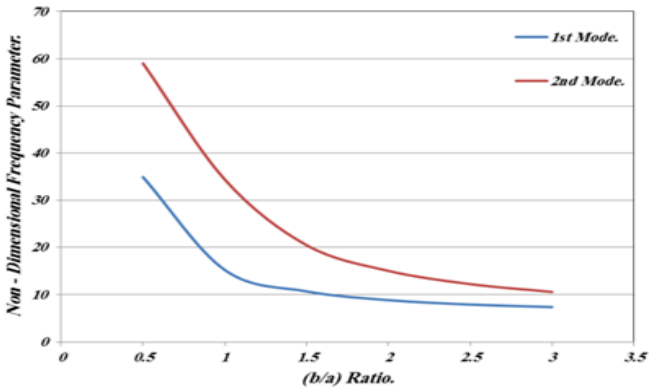


Fig. 14: The Comparison Between the First and Second Non-Dimensional Frequency Parameter Due to Change in (B/A) Ratio of Angle Ply Composite Plate [45º/-45º/45º/-45º] with SSSS Supporting.

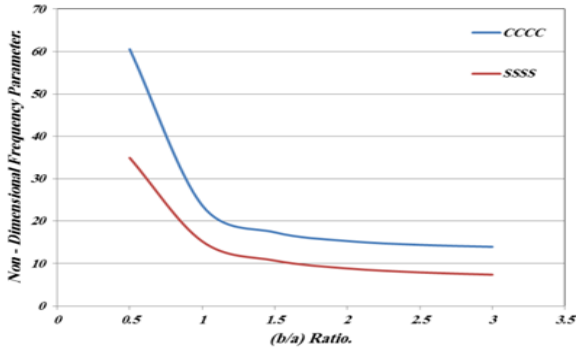


Fig.15: The Comparison between the First Non-Dimensional Frequency Parameter of CCCC and SSSS Supporting Due to Change in (B/A) Ratio of Angle Ply Composite Plate [45º/-45º/45º/-45º].

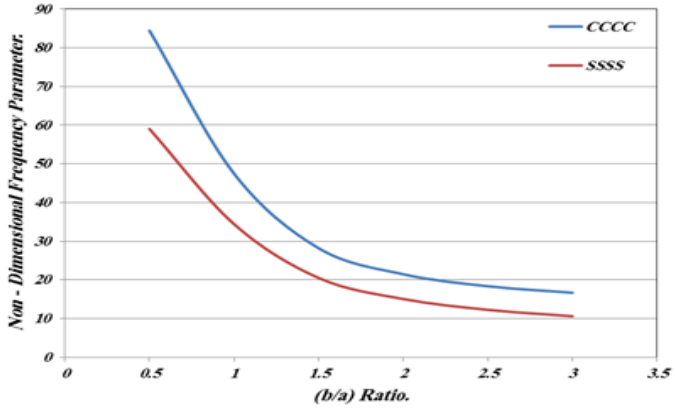


Fig.16: The Comparison between the Second Non-Dimensional Frequency Parameter of CCCC And SSSS Supporting Due to Change In (B/A) Ratio of Angle Ply Composite Plate [45º/-45º/45º/-45º].

2) Composite Spherical Shell:

For symmetrical cross ply composite spherical shell [0º/90º/0º/90º/0º], Fig.(17) and Fig.(18) show the comparisons between the non-dimensional frequency parameters of the first and second modes due to change in aspect ratio (b/a Ratio) when the supporting conditions is (CCCC) and (SSSS) respectively.

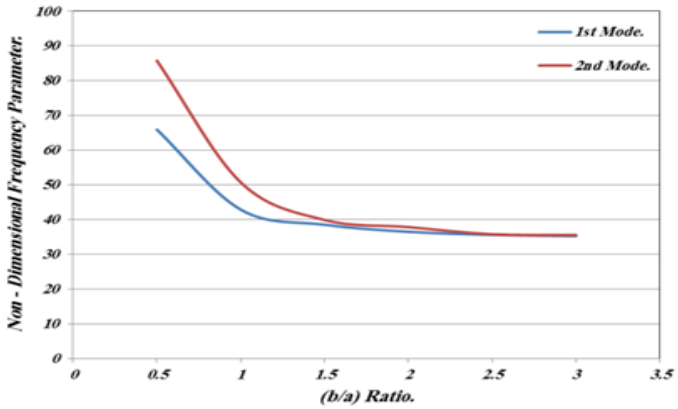


Fig. 17: The Comparison Between the First and Second Non-Dimensional Frequency Parameter Due to Change In (B/A) Ratio of Cross Ply Composite Spherical Shell [0º/90º/0º/90º/0º] with CCCC Supporting.

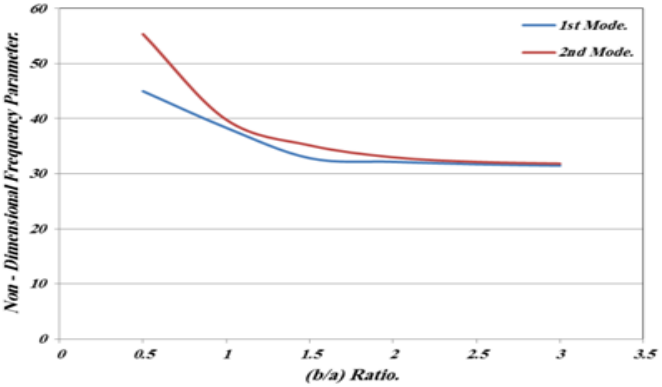


Fig. 18: The Comparison between the First and Second Non-Dimensional Frequency Parameter Due to Change in (b/a) Ratio of Cross Ply Composite Spherical Shell [0º/90º/0º/90º/0º] with SSSS Supporting.

Fig. (19) and Fig. (20) show the comparisons between the non-dimensional frequency parameters of (CCCC) and (SSSS) due to change in aspect ratio (b/a Ratio) .

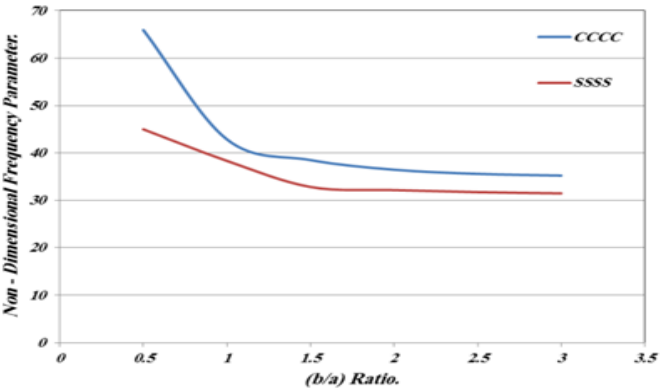


Fig. 19: The Comparison between the First Non-Dimensional Frequency Parameter of CCCC and SSSS Supporting Due to Change in (B/A) Ratio of Cross Ply Composite Spherical Shell [0º/90º/0º/90º/0º].

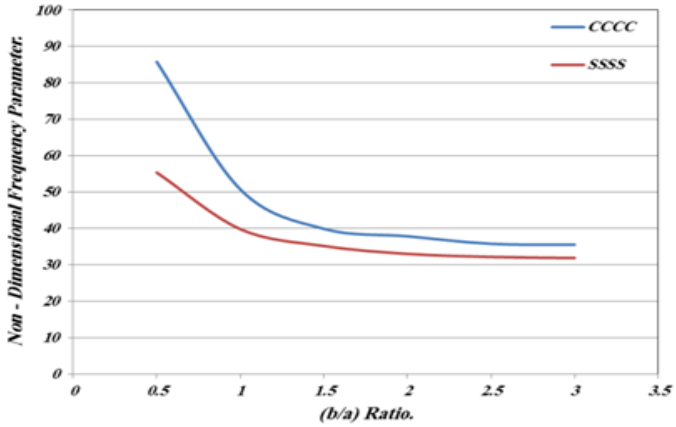


Fig. 20: The Comparison between the Second Non-Dimensional Frequency Parameter of CCCC and SSSS Supporting Due to Change in (B/A) Ratio Of Cross Ply Composite Spherical Shell [0º/90º/0º/90º/0º].

Also, Fig. (21)-Fig. (24) show the same comparisons for anti-symmetrical cross ply composite spherical shell [0º/90º/0º/90º].

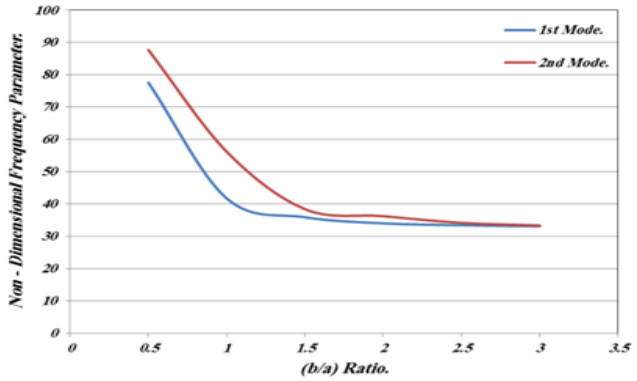


Fig. 21: The Comparison between the First and Second Non-Dimensional Frequency Parameter Due to Change in (B/A) Ratio of Cross Ply Composite Spherical Shell [0º/90º/0º/90º] with CCCC Supporting.

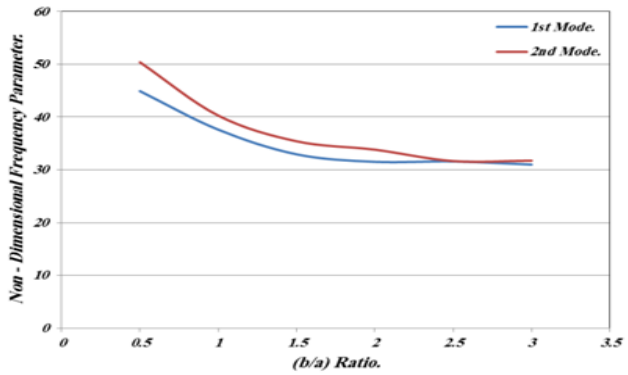


Fig. 22: The Comparison between the First and Second Non-Dimensional Frequency Parameter Due to Change in (B/A) Ratio of Cross Ply Composite Spherical Shell [0º/90º/0º/90º] with SSSS Supporting.

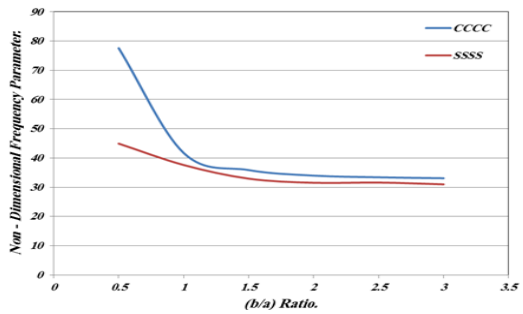


Fig. 23: The Comparison between the First Non-Dimensional Frequency Parameter of CCCC and SSSS Supporting Due to Change in (B/A) Ratio of Cross Ply Composite Spherical Shell [0º/90º/0º/90º].

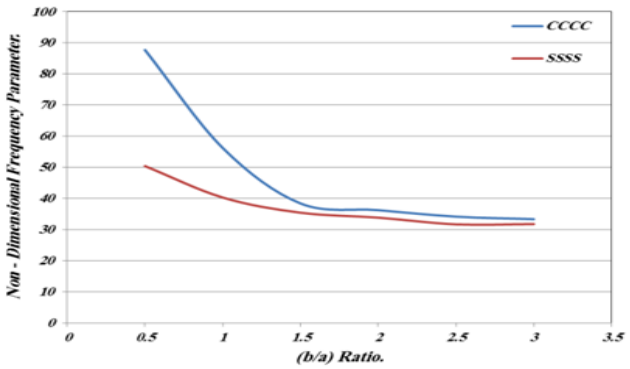


Fig. 24: The Comparison between the Second Non-Dimensional Frequency Parameter of CCCC And SSSS Supporting Due to Change in (B/A) Ratio of Cross Ply Composite Spherical Shell [0º/90º/0º/90º].

For symmetrical angle ply composite spherical shell [45o/-45o/45o/-45o/45o], Fig. (25) - Fig.(28) show the comparisons between the non-dimensional frequency parameters of the first and second modes due to change in aspect ratio (b/a Ratio) when the supporting conditions are (CCCC) and (SSSS).

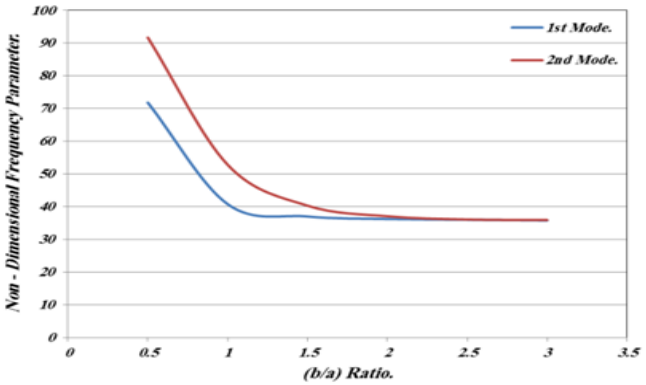


Fig. 25: The Comparison between the First and Second Non-Dimensional Frequency Parameter Due to Change in (B/A) Ratio of Angle Ply Composite Spherical Shell [45º/-45º/45º/-45º/45º] With CCCC Supporting.

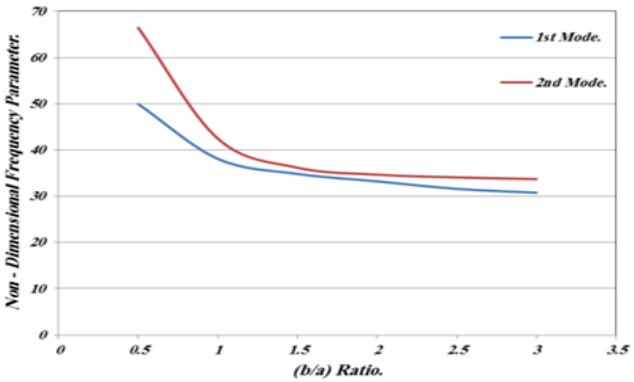


Fig.26: The Comparison between the First and Second Non-Dimensional Frequency Parameter Due to Change in (B/A) Ratio of Angle Ply Composite Spherical Shell [45º/-45º/45º/-45º/45º] With SSSS Supporting.

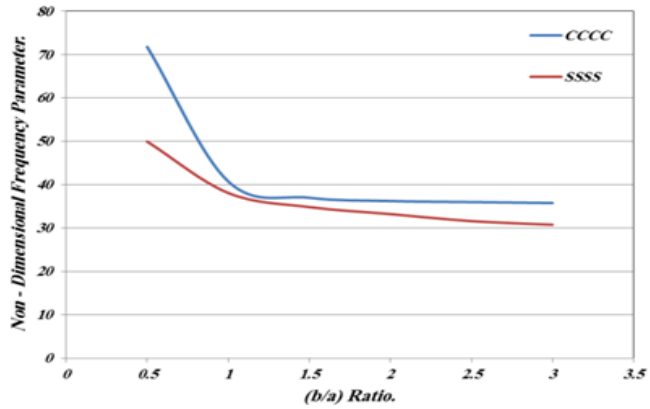


Fig. 27: The Comparison between the First Non-Dimensional Frequency Parameter of CCCC and SSSS Supporting Due to Change in (B/A) Ratio Of Angle Ply Composite Spherical Shell [45º/-45º/45º/-45º/45º].

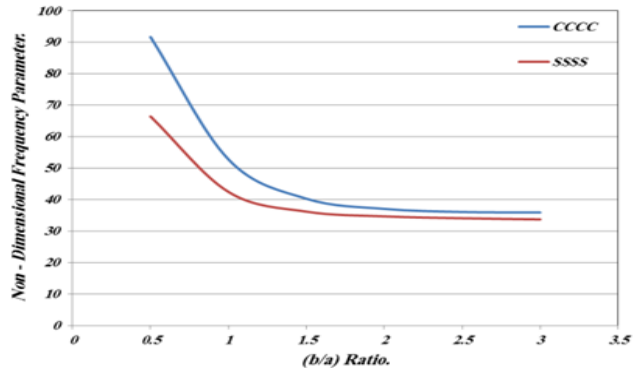


Fig. 28: The Comparison between the Second Non-Dimensional Frequency Parameter of CCCC And SSSS Supporting Due to Change in (B/A) Ratio of Angle Ply Composite Spherical Shell [45º/-45º/45º/-45º/45º].

Also, Fig. (29) - Fig. (32) show the same comparisons for anti-symmetrical cross ply composite spherical shell [45º/-45º/45º/-45º].

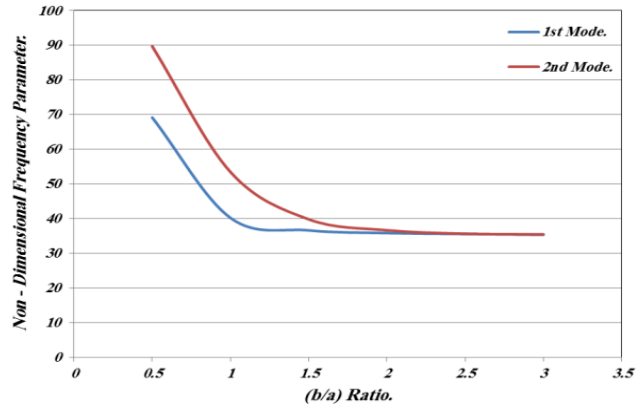


Fig. 29: The Comparison between the First and Second Non-Dimensional Frequency Parameter Due to Change In (B/A) Ratio of Angle Ply Composite Spherical Shell [45º/-45º/45º/-45º] With CCCC Supporting.

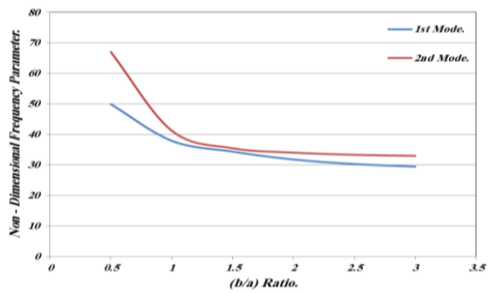


Fig. 30: The Comparison between the First and Second Non-Dimensional Frequency Parameter Due to Change in (B/A) Ratio of Angle Ply Composite Spherical Shell [45º/-45º/45º/-45º] With SSSS Supporting.

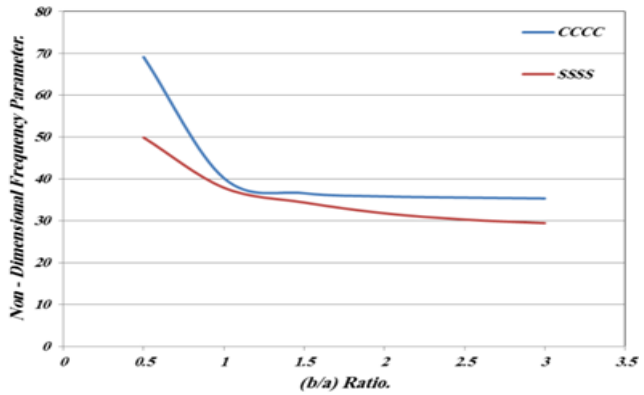


Fig. 31: The Comparison Between the First Non-Dimensional Frequency Parameter of CCCC and SSSS Supporting Due to Change in (B/A) Ratio Of Angle Ply Composite Spherical Shell [45º/-45º/45º/-45º].

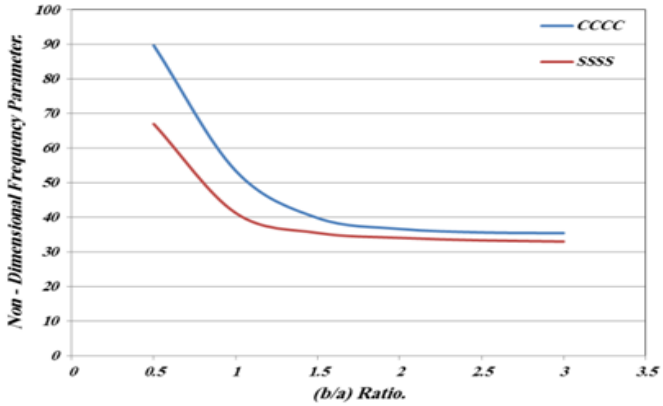


Fig. 32: The Comparison between the Second Non-Dimensional Frequency Parameter of CCCC and SSSS Supporting Due to Change in (B/A) Ratio of Angle Ply Composite Spherical Shell [45º/-45º/45º/-45º].

From figures (17) – (32), the following points can be seen:

1) The non-dimensional frequency parameter of (CCCC) is larger than that of (SSSS) for the first and second mode.
2) The effect of (b/a) ratio on the non-dimensional parameter of the first mode is larger than that of second mode when the boundary condition is (CCCC) or (SSSS).
3) In a large (b/a) ratio, the non-dimensional parameter of the second mode converges to that of first mode.
3) Comparison between the Composite Plate and Spherical Shell

Fig. (33) shows the comparisons between the non-dimensional frequency parameter of the first mode of the four types of composite plate and spherical shell when the boundary condition is (CCCC). Also, the comparisons between the non-dimensional frequency parameter of the second mode of the four types of composite plate and spherical shell is shown in Fig.(34) when the boundary condition is (CCCC). For (SSSS), Fig. (35) and Fig. (36) show the comparisons between the non-dimensional frequency parameter of the first and second mode of the cross and angle plies. From these figures:

1) The non-dimensional frequency parameter (first and second mode) of the composite plate is smaller than that of the composite spherical shell.
2) From the difference between the maximum and minimum values of the non-dimensional frequency parameter, the effect on the non- of (b/a) ratio dimensional frequency parameter of the composite plate is larger than that of the composite spherical shell.

Plate

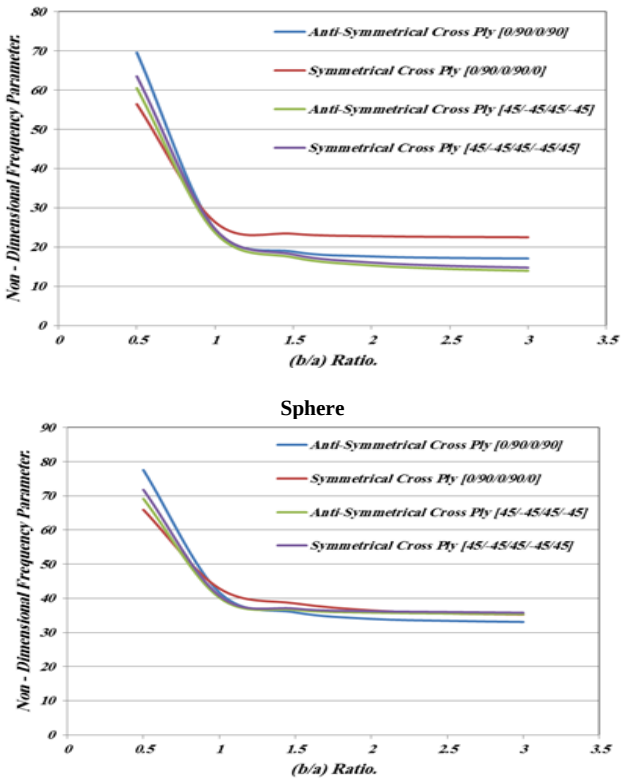


Fig. 33: The Comparison among Non- Dimensional Parameter of the First Mode for Different Arrangements of Composite Plates and Spherical Shells When the Supporting Is CCCC.

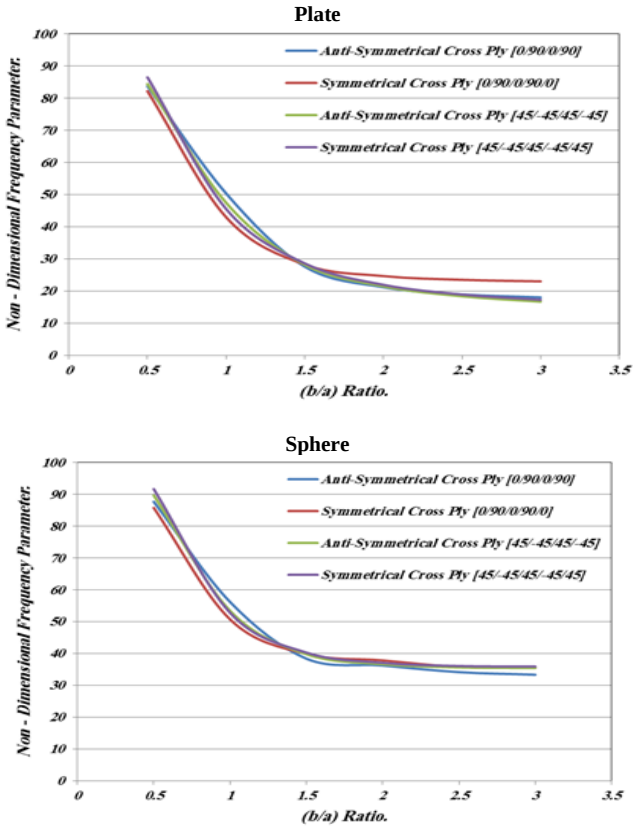


Fig. 34: The Comparison among Non- Dimensional Parameter of the Second Mode for Different Arrangements of Composite Plates and Spherical Shells when the Supporting is CCCC.

Plate

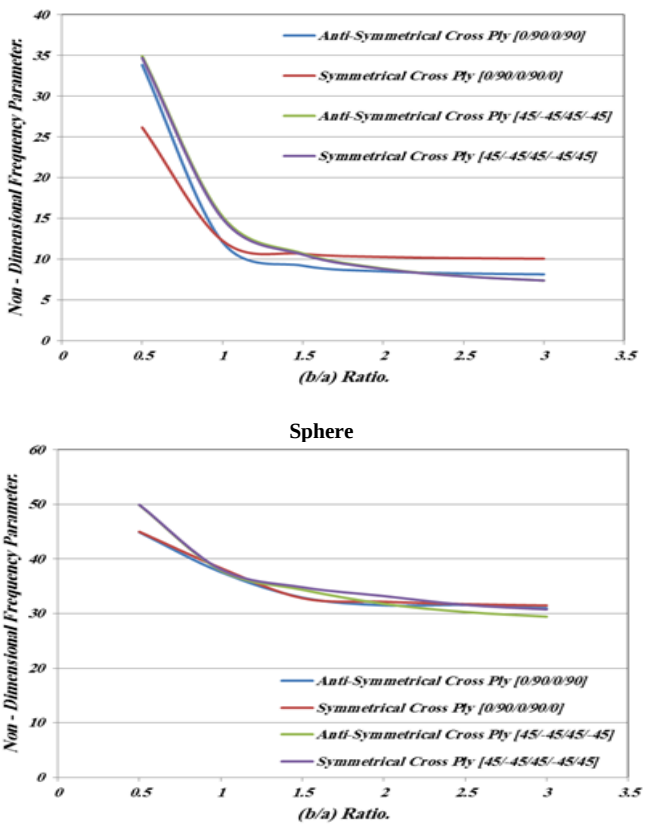


Fig. 35: The Comparison Among Non- Dimensional Parameter of the First Mode for Different Arrangements of Composite Plates and Spherical Shells When the Supporting is SSSS.

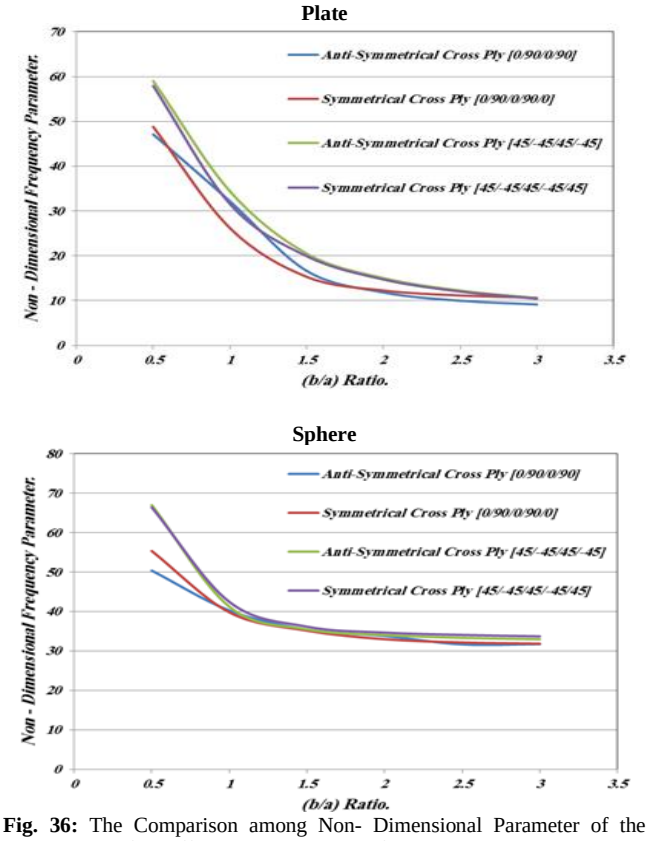


Fig. 36: The Comparison among Non- Dimensional Parameter of the Second Mode for Different Arrangements of Composite Plates and Spherical Shells When the Supporting Is SSSS.

6. Conclusion

From the results, the following points can be concluded:

1) For isotopic and composite plates, excellent agreements can be noted between the Fourier Ritz method and FEM with B-spline Rayleigh Ritz method.
2) The non-dimensional frequency parameter of (CCCC) is larger than that of (SSSS) for the first and second mode of composite plate and composite spherical shell.
3) The effect of (b/a) ratio on the non-dimensional parameter of the first mode is larger than that of second mode of composite plate and composite spherical shell. when the boundary condition is (CCCC) or (SSSS).
4) In a large (b/a) ratio, the non-dimensional parameter of the second mode converges to that of first mode of composite plate and composite spherical shell.
5) The non-dimensional frequency parameter (first and second mode) of the composite plate is smaller than that of the composite spherical shell.
6) From the difference between the maximum and minimum values of the non-dimensional frequency parameter, the effect of (b/a) ratio on the non-dimensional frequency parameter of the composite plate is larger than that of the composite spherical shell.

References

[1] Leissa, A. W., Lee, J. K., and Wang, A. J. 'Vibrations of cantilevered shallow cylindrical shells of rectangular planform', J. Sound Vib., vol. 78, pp. 311-328, 1981. https://doi.org/10.1016/S0022-460X(81)80142-3.

[2] Narita, Y., and Leissa, A. W. 'Vibrations of corner point supported shallow shells of rectangular planform', Earthq. Eng. Struct D, vol. 12, pp. 651-661, 1984. https://doi.org/10.1002/eqe.4290120506.

[3] Qatu, M. S., and Leissa, A. W. 'Free vibrations of completely free doubly curved laminated composite shallow shells', J. Sound Vib., vol. 151, pp. 9-29, 1991. https://doi.org/10.1016/0022-460X(91)90649-5.

[4] Lim, C. W., and Liew, K. M. A. 'pb-2 Ritz formulation for flexural vibration of shallow cylindrical shells of rectangular plan form', J. Sound Vib., vol. 73, pp. 343-375, 1994. https://doi.org/10.1006/jsvi.1994.1235.

[5] Young, P. G., and Dickinson, S. M. 'Vibration of a class of shallow shells bounded by edges described by polynomials, part I: theoretical approach and validation', J. Sound Vib., vol. 181, pp. 203-214, 1995. https://doi.org/10.1006/jsvi.1995.0135.

[6] Young, P. G., and Dickinson, S. M. 'Vibration of a class of shallow shells bounded by edges described by polynomials Part II: natural frequency parameters for shallow shells of various different plan forms', J. Sound Vib., vol. 181, pp. 215-230, 1995. https://doi.org/10.1006/jsvi.1995.0136.

[7] Qatu, M. S. 'Vibration studies on completely free shallow shells having triangular and trapezoidal plan forms', Appl Acoust, vol. 44, pp. 215-231, 1995. https://doi.org/10.1016/0003-682X(94)00020-V.

[8] Qatu, M. S. 'Vibration analysis of cantilevered shallow shells with triangular and trapezoidal plan forms', J. Sound Vib., vol. 191, pp. 219-231, 1996. https://doi.org/10.1006/jsvi.1996.0117.

[9] Zhang, X. M., Liu, G. R., and Lam, K. Y. 'Frequency analysis of cylindrical panels using a wave propagation approach', Appl. Acoust, vol. 62, pp. 527-543, 2001. https://doi.org/10.1016/S0003-682X(00)00059-1.

[10] Qatu, M. S. 'Effect of in plane edge constraints on natural frequencies of simply supported doubly curved shallow shells', Thin-Wall Struct., vol. 49, pp. 797-803, 2011. https://doi.org/10.1016/j.tws.2011.01.001.

[11] Monterrubio, L. E. 'Free vibration of shallow shells using the Rayleigh—Ritz method and penalty parameters', Proc. Inst. Mech. Eng., Part C, J. Mech. Eng. Sci., vol. 223, pp. 2263-2272, 2009. https://doi.org/10.1243/09544062JMES1442.

[12] Qatu, M. S., and Asadi, E. 'Vibration of doubly curved shallow shells with arbitrary boundaries', Appl. Acoust., vol. 73, pp. 21-27, 2012. https://doi.org/10.1016/j.apacoust.2011.06.013.

[13] Liew, K. M., and Lim, C. W. 'A higher-order theory for vibration analysis of curvilinear thick shallow shells with constrained boundaries', J. Vib. Control, vol. 1, pp. 15-39, 1995.

[14] Liew, K. M., and Lim, C. W. 'A higher-order theory for vibration of doubly curved shallow shells', J. Appl. Mech., vol. 63, pp. 587-593, 1996. https://doi.org/10.1115/1.2823338.

[15] Liew, K. M., Lim, C. W. 'Vibration of thick doubly-curved stress-free shallow shells of curvilinear plan form', J. Eng. Mech., vol. 123, pp. 413-421, 1997. https://doi.org/10.1061/(ASCE)0733-9399(1997)123:5(413).

[16] Matsunaga, H. 'Vibration and stability of thick simply supported shallow shells subjected to in-plane stresses', J. Sound Vib., vol. 225, pp. 41-60, 1999. https://doi.org/10.1006/jsvi.1999.2234.

[17] Bhimaraddi, A. 'Free vibration analysis of doubly curved shallow shells on rectangular planform using three-dimensional elasticity theory', Int. J. Solids Struct., vol. 27, pp. 897-913, 1991. https://doi.org/10.1016/0020-7683(91)90023-9.

[18] Liew, K. M., and Lim, C. W. 'A Ritz vibration analysis of doubly-curved rectangular shallow shells using a refined first-order theory', Comput. Methods Appl. Mech. Eng. vol. 127, pp. 145-162, 1995. https://doi.org/10.1016/0045-7825(95)00837-1.

[19] Chakravorty. D., and Bandyopadhyay, J. N. 'On the free vibration of shallow shells', J. Sound Vib., vol. 185, pp. 673-684, 1995. https://doi.org/10.1006/jsvi.1995.0408.

[20] Liew, K. M., and Lim, C. W. 'Vibration studies on moderately thick doubly-curved elliptic shallow shells', Acta. Mech., vol. 116, pp. 83-96, 1996. https://doi.org/10.1007/BF01171422.

[21] Lim, C. W., Li, Z. R., and Wei, G. W. 'DSC-Ritz method for high-mode frequency analysis of thick shallow shells', Inter J. Numer. Methods Eng., vol. 62, pp. 205-232, 2005. https://doi.org/10.1002/nme.1179.

[22] Qatu, M. S. 'Natural vibration of free, laminated composite triangular and trapezoidal shallow shells', composites structure, vol. 31, pp. 9–19, 1995.

[23] Khdeir, A. A., Reddy, J. N. 'Free and forced vibration of cross-ply laminated composite shallow arches', Int. Solids Structure, vol. 34, pp. 1217–34, 1997. https://doi.org/10.1016/S0020-7683(96)00095-9.

[24] Soldatos, K. P., and Shu, X. P. 'On the stress analysis of cross-ply laminated plates and shallow shell panels', Composites Structure, vol. 46, pp. 333–44, 1999. https://doi.org/10.1016/S0263-8223(99)00061-6.

[25] Reddy, J. N. 'Mechanics of laminated composite plates and shells: theory and analysis. 2nd', CRC Press, 2004. https://doi.org/10.1201/b12409.

[26] Qatu, M. S. 'Vibration of laminated shells and plates', San Diego: Elsevier, 2004.

[27] Ferreira, AJM., Castro, L. M., Bertoluzza, S. 'A wavelet collocation approach for the analysis of laminated shells', Compos Part B: Eng., vol. 42, pp. 99-04, 2011. https://doi.org/10.1016/j.compositesb.2010.06.003.

[28] Ferreira, AJM., Carrera, E., Cinefra, M., and Roque, CMC. 'Analysis of laminated doubly curved shells by a layerwise theory and radial basis functions collocation, accounting for through-the-thickness deformations', Compute Mech., vol. 48, pp. 13-25, 2011. https://doi.org/10.1007/s00466-011-0579-4.

[29] Qatu, M. S., and Asadi, E. 'Vibration of doubly curved shallow shells with arbitrary boundaries', Appl. Acoustic., vol. 73, pp. 21–7, 2012. https://doi.org/10.1016/j.apacoust.2011.06.013.

[30] Sayan, B. and Bhavani, V. 'Mechanical properties of hybrid composites using finite element method-based micromechanics', composites: part B, vol. 58, pp. 318-327, 2014.

[31] Guoyong, J., Shuangxia S., Zhu S., Shouzuo, L. and Zhigang, L. 'A modified Fourier-Ritz approach for free vibration analysis of laminated functionally graded shallow shells with general boundary conditions', International Journal of Mechanical Sciences, http://dx.doi.org/10.1016 j ijmecsci...02.006, 2015.

[32] Qingshan, W., Dongyan, S., Fuzhen, P., and Qian L. 'Vibrations of composite laminated circular panels and shells of revolution with general elastic boundary conditions via fourier-ritz method', http://dx.doi.org/10.1515/cls accepted, 2016.

[33] Wang, Q., Cui, X., Qin, B., and Liang, Q. 'Vibration analysis of the functionally graded carbon nanotube reinforced composite shallow shells with arbitrary boundary conditions, composite structures', http://doi.org/10.1016/j. compstruct, vol. 9, p.p. 43, 2017.

[34] Guoyong, J., Tiangui, Y., and Zhu S. 'Structural Vibration: A Uniform Accurate Solution for Laminated Beams, Plates and Shells with General Boundary Conditions', Science Press, Beijing and Springer-Verlag Berlin Heidelberg, 2015.

[35] Singiresu, S. R. 'Mechanical Vibrations', Fifth Edition, Pearson Education, Inc., publishing as Prentice Hall, 1 Lake Street, Upper Saddle River, NJ 07458, 2004.

[36] Wang 'vibration of thin skew fiber reinforced composite laminated', Journal of Sound and Vibration, vol. 201, pp. 335–352, 1997. https://doi.org/10.1006/jsvi.1996.0745.